

Origin of Pacific Multidecadal Variability in Community Climate System Model, Version 3 (CCSM3): A Combined Statistical and Dynamical Assessment

YAFANG ZHONG AND ZHENGYU LIU

Center for Climate Research, University of Wisconsin—Madison, Madison, Wisconsin

R. JACOB

Argonne National Laboratory, Department of Energy, Argonne, Illinois

(Manuscript received 17 October 2006, in final form 24 April 2007)

ABSTRACT

Observations indicate that Pacific multidecadal variability (PMV) is a basinwide phenomenon with robust tropical–extratropical linkage, though its genesis remains the topic of much debate. In this study, the PMV in the Community Climate System Model, version 3 (CCSM3) is investigated with a combined statistical and dynamical approach. In agreement with observations, the modeled North Pacific climate system undergoes coherent multidecadal atmospheric and oceanic variability of a characteristic quasi-50-yr time scale, with apparent connections to the tropical Indo-Pacific.

The statistical assessment based on the CCSM3 control integration cannot exclusively identify the origin of the modeled multidecadal linkage, while confirming the two-way interactions between the tropical and extratropical Pacific. Two sensitivity experiments are performed to further investigate the origin of the PMV. With the atmosphere decoupled from the tropical ocean, multidecadal variability in the North Pacific climate remains outstanding. In contrast, without midlatitude oceanic feedback to atmosphere, an experiment shows much reduced multidecadal power in both extratropical atmosphere and surface ocean; moreover, the tropical multidecadal variability seen in the CCSM3 control run virtually disappears. The combined statistical and dynamical assessment supports a midlatitude coupled origin for the PMV, which can be described as follows: extratropical large-scale air–sea interaction gives rise to multidecadal variability in the North Pacific region; this extratropical signal then imprints itself in the tropical Indo–Pacific climate system, through a robust tropical–extratropical teleconnection. This study highlights a midlatitude origin of multidecadal tropical–extratropical linkage in the Pacific in the CCSM3.

1. Introduction

Historical data of the twentieth century have revealed covarying multidecadal variability in the atmospheric and oceanic components of North Pacific climate system (Minobe 1997; Mantua et al. 1997; Enfield and Mestas-Nunez 1999; Deser et al. 2004). These variations are evident in several key indices of the North Pacific climate system, including the North Pacific index (NPI; Trenberth and Hurrell 1994) and the Pacific decadal oscillation (PDO) index (Mantua et al. 1997). The NPI is defined as the area-averaged sea level pressure (SLP) over the region 30°–65°N, 160°E–140°W

and measures the strength of the Aleutian low pressure cell during the boreal winter season. The PDO index is used to depict the decadal-time-scale-dominated variability in the North Pacific Ocean, and is defined as the leading principal component of monthly sea surface temperature (SST) in the Pacific poleward of 20°N. Both indices exhibit substantial multidecadal variability, sharing the three marked regime shifts in 1920s, 1940s, and 1970s (see Fig. 1 of Deser et al. 2004 and Fig. 1 of Latif 2006). Such Pacific multidecadal variability (PMV), however, is not unique to the twentieth century. Evidence for additional multidecadal regime shifts in the previous three centuries was demonstrated with a tree-ring reconstruction of NPI extending back to the seventeenth century in a recent study of D'Arrigo et al. (2005).

Various hypotheses of PMV have been put forward. One school of thought highlights the importance of in-

Corresponding author address: Yafang Zhong, Center for Climate Research, Department of Atmospheric and Oceanic Sciences, University of Wisconsin—Madison, Madison, WI 53706.
E-mail: yafangzhong@wisc.edu

trinsic midlatitude processes. This can be subdivided into uncoupled, unstable coupled, and stable coupled midlatitude origins. An influential theory of the uncoupled origin is the simple stochastic climate model described by Hasselmann (1976). In this prototype model, the midlatitude ocean mixed layer integrates atmospheric white noise forcing and yields a red spectrum for ocean temperature. With the inclusion of oceanic dynamics such as mean advection (Saravanan and McWilliams 1998) and midlatitude Rossby wave propagation (Frankignoul et al. 1997; Jin 1997), the stochastic climate model has been extended to explain enhanced oceanic variability at decadal–multidecadal time scales by considering temporally stochastic, but spatially coherent atmospheric forcing. These complex versions of the Hasselmann hypothesis are termed “spatial resonance.”

Unstable coupled midlatitude origin was introduced in the seminal study of Latif and Barnett (1994), who described the midlatitude decadal-scale variability as an oscillatory cycle involving strong oceanic feedback to the atmosphere, with decadal peaks anticipated to exist in both the ocean and atmosphere. The key processes include the slow ocean dynamic adjustment to basin-scale wind stress curl forcing and a strong response in wind stress curl field to midlatitude SST. A major weakness of this theory rests in the unrealistically large atmospheric response to underlying midlatitude SST required to reverse the phase of oscillation (Kushnir et al. 2002).

Using a conceptual midlatitude coupled model, Neelin and Weng (1999) examined the possibility of a stable coupled origin and concluded a weak oceanic feedback to the atmosphere could considerably enhance a decadal oceanic spectral peak caused by spatial resonance. Eigenvalue analysis of the same conceptual model by Weng and Neelin (1999) found that coupling creates an oscillatory interdecadal mode that is intrinsically stable and may be maintained by atmospheric stochastic forcing. Such an effect of a modest feedback to atmosphere was claimed to be crucial for the prominent decadal–multidecadal variability in the North Pacific Ocean from a long integration of the Community Climate System Model, version 2 (CCSM2; Kwon and Deser 2007). All of the three above origins are intrinsic to the North Pacific region, with the tropical Pacific playing a role of passive response (Kleeman et al. 1999; Solomon et al. 2003; McPhaden and Zhang 2002).

Another school of thought suggests a critical role of the tropical Pacific in the genesis of PMV. For instance, a closed loop of tropical–extratropical interaction has been proposed to explain the basinwide decadal-scale variability in the Pacific (Gu and Philander 1997).

Strong positive feedback in the tropical Pacific fuels the variability of such tropical–extratropical coupled origin, which is expected to have a basinwide signature in both the atmosphere and ocean. Alternatively, tropical decadal-scale variability may arise from an intrinsic tropical origin in the form of a delayed oscillator similar to that responsible for El Niño–Southern Oscillation (ENSO) interannual variability, but involving slower Rossby waves either at higher latitudes (Kirtman 1997) or of higher vertical mode number (Liu et al. 2002, hereafter L02). Via the atmospheric bridge, such intrinsic tropical variability imprints itself in the North Pacific atmospheric circulation, thereafter leading to preferred oceanic multidecadal variability superposing on a red-noise background (Newman et al. 2003; An and Wang 2005).

Several questions on the origin of PMV are yet to be asked. First of all, does the extratropical atmosphere show any preference for multidecadal variability beyond a pure stochastic process? If yes, does it originate from remote tropical teleconnective forcing? To verify an active role of the tropics as in tropical–extratropical coupled or intrinsic tropical origin, a tropical–extratropical linkage must be established at a multidecadal time scale. In the absence of such a constructive role of the tropics, the existence of a multidecadal signal in the North Pacific atmospheric circulation may be a hint of a midlatitude coupled origin; otherwise, the oceanic multidecadal variability probably arises from stochastic atmospheric forcing of uncoupled origin.

In reality, the PMV is not limited to the North Pacific region, but is rather a basinwide phenomenon (Chao et al. 2000; Linsley et al. 2000). Through a comprehensive and physically based analysis of multiple observational datasets, Deser et al. (2004) provided evidence for substantial multidecadal variations in a tropical coupled climate system that correspond well with those in NPI during the twentieth century. By comparing simple difference maps between epochs of high and low NPI for numerous climate variables in the tropical Indo-Pacific, they identified some robust features of tropical linkage to North Pacific multidecadal climate variability. To further characterize this multidecadal linkage, they demonstrated a suite of selected regional climate anomaly records over the tropical Indo-Pacific that is coherent with the NPI.

Weak as it may be, the tropical–extratropical linkage at a multidecadal time scale has implications for the origin of PMV. Based on such weak yet robust linkage, Deser et al. (2004) intended to lend support to tropics-induced multidecadal variations in NPI; in opposition, Enfield and Mestas-Nunez (1999) and Latif (2006) accentuated the weakness of the tropical multidecadal

signal and excluded the tropics as a main contributor to a bulk of multidecadal variability in the North Pacific.

Coherent multidecadal variability in the tropics and North Pacific does not necessarily signal a tropical origin. Even though the tropical-induced “atmospheric bridge” (Alexander et al. 2002) is well known as the most effective communicator between the tropics and North Pacific climate system, the extratropical-initiated “seasonal footprinting mechanism” (SFM; Vimont et al. 2001, 2003) and coastal Kelvin waves (Lynse et al. 1997) may lead to such coherent variability as well. With observational datasets or output from model control integration, the effective origin of PMV is hard to distill among the numerous candidates as previously discussed, partially because of the difficulty in unraveling the complex tropical–extratropical interactions.

Recently, L02 and Wu et al. (2003, hereafter W03) studied the origin of PDO using a modeling surgery strategy in a fully coupled general climate model (GCM): the Fast Ocean Atmosphere Model (FOAM). By performing sensitivity experiments with ocean–atmosphere coupling decoupled in specific regions, they were able to identify the origin of PDO. This work is an extension of L02 and W03, with a further study in the Community Climate System Model, version 3 (CCSM3).

The origin of the PMV simulated by the CCSM3 control integration is explored with a combined statistical and dynamical approach. We will first attempt to investigate the PMV using statistical methods on the control run. The advantage of this approach is that the statistical analysis can be readily compared with the observation. As will be shown later, the CCSM3 yields a multidecadal tropical–extratropical linkage similar to Deser et al. (2004). The statistical assessment, however, cannot exclusively identify the origin of such a linkage, while confirming the two-way interactions between the tropical and extratropical Pacific (Newman et al. 2003; Vimont et al. 2003). The dynamical approach of L02 and W03 is thus adopted to clearly identify the origin of PMV. Our combined statistical and dynamical assessment suggests the PMV in CCSM3 arises from large-scale air–sea interaction at midlatitudes; this intrinsic extratropical variability in turn creates coherent variations in the tropical climate system, thus establishing a robust tropical–extratropical linkage. These conclusions from the CCSM3 are consistent with the findings of L02 and W03.

The paper is laid out as follows. Section 2 contains descriptions of CCSM3 and sensitivity experiments, analysis procedures, as well as the observational dataset. In section 3, the PMV in CCSM3 control integration is evaluated by comparison to its observational

counterpart. Section 4 is devoted to statistical assessment of possible PMV origins in terms of CCSM3 control integration. The origin is investigated further in section 5 by performing sensitivity experiments. Sections 6 and 7 are the discussion and summary, respectively.

2. Model and experiment description, analysis procedures, and observational dataset

CCSM3 is a state-of-art global climate model consisting of four components for the atmosphere, ocean, sea ice, and land surface linked through a coupler (Collins et al. 2006). CCSM3 at resolution T31x3 is employed in this study for its computational efficiency and its reasonable simulation comparable to higher-resolution CCSM3 results (Yeager et al. 2006). The atmospheric component of CCSM3 at T31x3 is the Community Atmosphere Model, version 3 (CAM3) at T31 resolution, which has 26 levels in the vertical. The ocean model is the Parallel Ocean Program (POP, version 1.4.3) in spherical polar coordinates with a dipole grid and has a nominal horizontal resolution of 3°. The vertical dimension is a depth coordinate with 25 levels extending to 4.75 km. The sea ice model is the Community Sea Ice Model, version 5 (CSIM5), a dynamic–thermodynamic model with the same horizontal grid as the ocean model. The land component of the CCSM3 is the Community Land Model, version 3 and is integrated at the same horizontal grid as the atmospheric component model. Further details on model configuration and the solution aspects at T31x3 are provided in Collins et al. (2006) and Yeager et al. (2006), respectively. A comprehensive exhibition of model climatology is available online at <http://www.cesm.ucar.edu/experiments/ccsm3.0/>.

CCSM3 at T31x3 has been integrated under the present-day atmospheric conditions. The ocean component was initialized with *World Ocean Atlas 1998* climatology and the Polar Science Center Hydrographic Climatology Arctic data. Following a one-time non-physical correction of North Sea salinities at year 133, the model integration has been extended to year 880 without flux adjustment showing no apparent climate drift. Analyses of this control integration are based on the last 400 yr of simulation.

In addition to the CCSM3 control integration (named CTRL), a couple of sensitivity experiments are performed to identify the origin of PMV. The modeling strategy used is partial coupling (PC; L02 and W03), which deactivates atmosphere–ocean coupling in specified regions while retaining it elsewhere. In the decoupled regions, the atmosphere “sees” prescribed SST from the seasonal climatology of CTRL and is there-

fore not affected by the SST anomalies predicted by the model's ocean component. Specifically, the coupler component calculates two sets of air–sea interfacial fluxes, including heat flux, water flux, and wind stress. One set of fluxes is calculated with the ocean-component-predicted SST and sent to the ocean component; the other set is calculated with the climatological SST and sent to the atmosphere component. For comparison, in the control integration or in fully coupled regions, only one set of flux is calculated with the ocean-component-predicted SST and is sent to both atmosphere and ocean components. Thereby, in the decoupled regions, the ocean is still driven by heat flux and wind stress anomalies, rather than purely climatological fluxes. In this work, the PC approach has been applied to the tropics and extratropics, named experiments PC-ET and PC-T, respectively. Both experiments were started from the CCSM3 control run at year 651 and integrated for 400 yr without flux correction.

Most of the analyses presented here are performed with annual mean data. All time series have been first detrended before further analysis. To focus on multidecadal time scale, low-pass filtering is applied prior to EOF analysis to retain variability longer than 20 yr (Zhang et al. 1997; Pierce et al. 2000; Vimont et al. 2002); meanwhile, the temporal evolution of such EOF modes is obtained by projecting raw (unfiltered) data onto the EOF spatial patterns following Saravanan and McWilliams (1997). In checking the physical consistency of several quantities, “associated pattern” refers to the projection of a climate field onto a selected index after 20–80-yr band filtering; projecting the unfiltered field onto the associated pattern, in turn, derives its temporal evolution, or “associated time series” (Latif and Barnett 1996). Power spectrum analysis, an objective tool to illustrate the characteristic time scale, is then applied to the projection time series. The unfiltered data, rather than filtered data, are used to ensure that any peaks in the spectrum are not simply an artifact of the time filter (Saravanan and McWilliams 1997; Wu et al. 2003). All power spectra and squared coherence are obtained through multitaper spectrum analysis (Mann and Lees 1996), and the resultant power spectra are further confirmed by those derived by the Fourier transform of autocorrelation function (not shown). Statistical significance of all the regression/correlation coefficients and variance ratio is assessed with a two-tailed Student's t test and F test, respectively, taking into account temporal autocorrelation following Bretherton et al. (1999).

The observational SST dataset used is the Kaplan extended SST dataset on a 5° latitude–longitude grid from 1856 to 2005 (Kaplan et al. 1998).

SST standard deviation

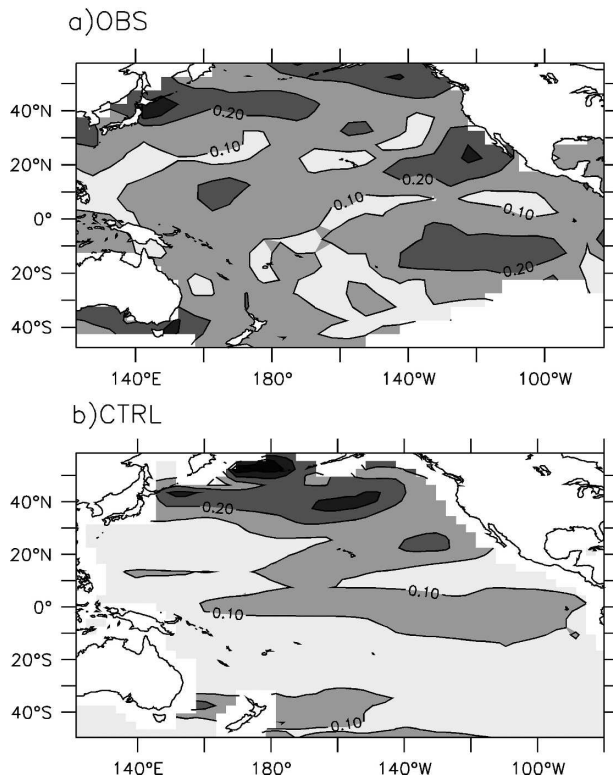


FIG. 1. Spatial distribution of standard deviation of 20-yr low-pass-filtered SST in (a) Kaplan observation and (b) CTRL. Contour interval (CI) is 0.1°C .

3. PMV in CCSM3

The PMV in the CTRL is compared to the observation. Figure 1 displays the spatial distributions of the observed and modeled multidecadal SST standard deviations in the Pacific. The observation exhibits the strongest signal in the mid- to high latitudes of the North Pacific, the off-equatorial eastern Pacific, and to the east of southeastern Australia; a slightly weaker signal occurs in the western equatorial Pacific. In contrast to such a somewhat interhemispheric symmetric distribution of real signal, the multidecadal variability in CTRL is dominated by North Pacific variability. The modeled multidecadal variability has magnitudes comparable to the observation in the North Pacific, but considerably weaker (<50%) in the tropical and South Pacific.

We apply standard EOF analysis to the multidecadal SST variability poleward of 20°N in the North Pacific region. Explaining 48% of the total multidecadal variance, the leading mode in CTRL (Fig. 2a) appears very similar to the classical PDO, exhibiting a basinwide

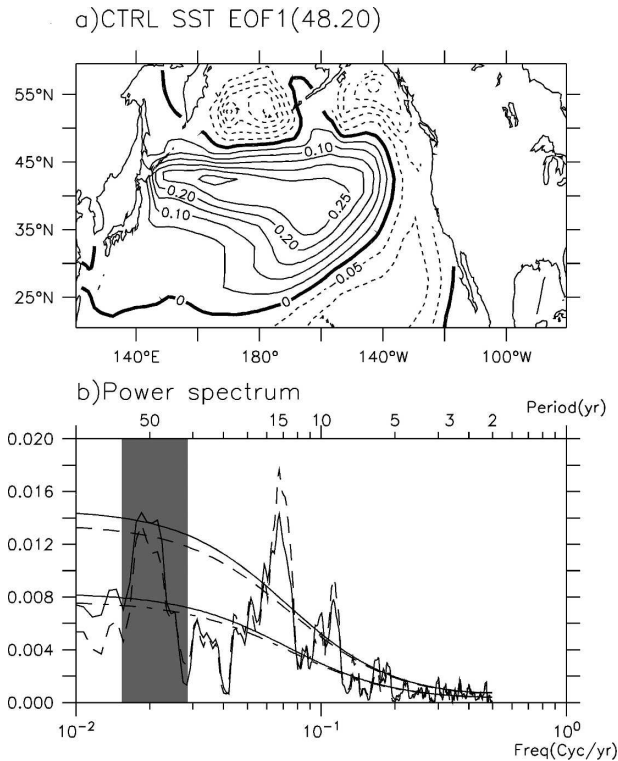


FIG. 2. (a) Leading EOF pattern of 20-yr low-pass-filtered SST anomalies in the North Pacific (20° – 60° N) from CTRL. CI = 0.05°C . Value in parentheses denotes percentage of total variance explained. (b) Power spectra of the projected time series (normalized) associated with this EOF pattern (solid) and unfiltered SST averaged over the loading center (35° – 45° N, 140° – 140° W; dashed). The 90% and 50% confidence levels are indicated. The quasi-50-yr frequency band is highlighted with shading.

horseshoe-like structure with one sign in the central and western North Pacific and an opposite sign in the surrounding region (Mantua et al. 1997). The primary center of action occurs along 40° N, agreeing well with the observation (Enfield and Mestas-Nunez 1999). The power spectrum of the projection time series associated with this mode exhibits a peak at quasi-50-yr time scale, which lies within the uncertainty of that inferred from observational multidecadal variability.

To ensure the quasi-50-yr peak is not simply an artifact of the low-pass filter, the spectra of the area-averaged SST over the loading center of the EOF pattern is also computed. It exhibits the same multidecadal peak that is significant at the 90% confidence level (dashed in Fig. 2b). Coherence analysis shows that SSTs along the Kuroshio Extension (KOE) and the central North Pacific (CNP) vary coherently at multidecadal time scale (not shown), which is consistent with the elongated center of multidecadal mode along 40° N in Fig. 2a and differs from the predominant KOE variabil-

ity in CCSM2 (Kwon and Deser 2007). In addition to the quasi-50-yr peak, a quasi-15-yr decadal peak stands out in both of the SST spectra, indicative of a decadal oscillation superimposing. A similar superimposing in the observation has been noticed by Minobe (1999). The fact that the projection time series captures the decadal oscillation suggests the spatial structure of the decadal oscillation resembles that of PMV, consistent with the notion that decadal–multidecadal variability in the North Pacific SST is driven by the atmosphere at first order (Hasselmann 1976; Frankignoul et al. 1997; Barsugli and Battisti 1998). Similar decadal peaks have been reported and investigated by many theoretical and modeling studies that fostered much of our knowledge on Pacific decadal–multidecadal variability, especially on the underlying mechanisms. Such decadal oscillation, however, is not the focus of this study and therefore will not be discussed in detail.

We also inspect the atmospheric association with the multidecadal SST mode in CTRL. The associated pattern of extratropical SLP (Fig. 3a) resembles the Northern Hemisphere annular mode (NAM; Thompson and Wallace 2000), exhibiting a seesaw between the midlatitudes and the polar region. The midlatitude region is dominated by one center over the North Pacific sector and another center over the North Atlantic sector. The NAM is substantially different from the Pacific–North America (PNA) pattern that is associated with the PMV in observation (Mantua et al. 1997; Minobe 2000). Indeed, the NAM and PNA correspond respectively to the first and second leading EOF patterns of annual SLP anomalies poleward of 20° N in CTRL (not shown). As in observation, the NPI, which captures the overall strengthening and weakening of Aleutian low, is more of an index for the PNA than for the NAM (Quadrelli and Wallace 2004). Shown in Fig. 3b is the power spectrum of the projection time series associated with the NAM, exhibiting a quasi-50-yr peak superimposing on the largely white noise background. The same peak is also evident in the power spectrum of the leading principal component of the unfiltered SLP field that corresponds to the NAM (not shown). For comparison, the multidecadal signal is expressed with the PNA in reality, as documented by the historical NPI (Deser et al. 2004).

The seasonality of the PMV has been examined with winter (December–January) and summer (June–August) data. While the SST signal persists throughout the year, the SLP expression of the PMV is appreciable only in winter, in agreement with the observation (Barlow et al. 2001; Minobe 2000).

To summarize, the CTRL simulated a PMV that has both oceanic and atmospheric expressions, as in obser-

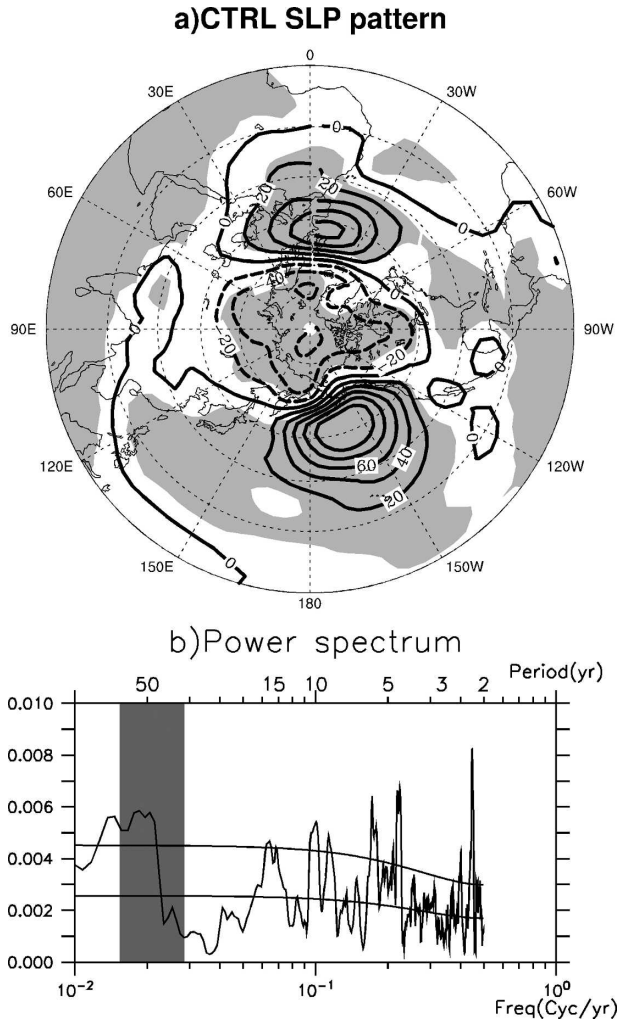


FIG. 3. (a) Regression of Northern Hemispheric SLP in CTRL onto the projection time series associated with the multidecadal SST mode in Fig. 2. All data are bandpass filtered to retain variability at a 20–80-yr time scale. The shading indicates regressions significant at a 90% confidence level. CI = 20 Pa. (b) Power spectrum of the projected time series (normalized) associated with the regression SLP pattern. This SLP time series is defined as “multidecadal index.” The 90% and 50% confidence levels are indicated. The quasi-50-yr frequency band is highlighted with shading.

vation. The modeled PMV, however, shows some discrepancies from the real PMV. First, the signal of PMV is considerably reduced in the tropical and South Pacific. Second, it is the NAM, unlike the PNA in reality, that is associated with the PMV. These model deficiencies should be cautioned when it comes to model illumination for reality. The genesis of the modeled multidecadal signal is explored in the following sections. For convenience, the projection time series associated with the NAM (Fig. 3) is defined as a “multidecadal index” after normalization; all associated patterns here-

after are derived in term of this index. The SLP time series, rather than the SST time series, is used following Deser et al. (2004), in that the extratropical atmosphere is more directly connected to the tropics than the North Pacific Ocean with respect to the PMV, as found out later in this study. In fact, the use of an SST time series yields essentially the same results.

4. The origin of PMV: Inference from the control simulation

What causes the multidecadal variability in the atmospheric circulation of Northern Hemisphere (NH) extratropics? Does it originate from midlatitude air–sea interaction or remote tropical teleconnective forcing? We will first attempt to address these questions by using statistical methods on the control run.

a. Multidecadal tropical–extratropical linkage

First, we investigate the possibility of tropical-driven PMV. Equivalently, is the tropical–extratropical or intrinsic tropical origin discussed in the introduction relevant to the PMV in CTRL?

Following the observational study of Deser et al. (2004), the connections between the extratropical multidecadal variability and multiple tropical climate fields are carefully examined. Figure 4 shows the associated patterns of tropical variables, including SST, SLP, precipitation, and total cloud cover. These patterns were obtained by projection of tropical variables onto the multidecadal index after 20–80-yr band filtering. Corresponding with an anomalously high pressure over the North Pacific sector (Fig. 3a) and warm western-central North Pacific (Fig. 2a), cool SST anomalies occur in most of the tropical Indo-Pacific, with maximums in the northern, central, and eastern tropical Pacific; weak and insignificant warm anomalies are found over the southeastern tropical Indian Ocean and to the east of the South Pacific convergence zone (SPCZ) (Fig. 4a). The associated SLP pattern (Fig. 4b) takes on a Southern Oscillation–like pattern, featuring a seesaw between the Indo-Australian and eastern regions of the tropical Pacific. The accompanying changes in precipitation and cloud cover are characterized by poleward shifts of the Pacific ITCZ and SPCZ away from the anomalous cooling along the equator. Reduced precipitation and cloud cover occur over the regions to the south of the Pacific ITCZ; enhanced precipitation and cloud cover are found to the south of the SPCZ (Figs. 4c,d). As a result, the tropical climate fields systematically exhibit apparent connections to the extratropical multidecadal variability, in agreement with the observational PMV of Deser et al. (2004).

CTRL: associated tropical patterns

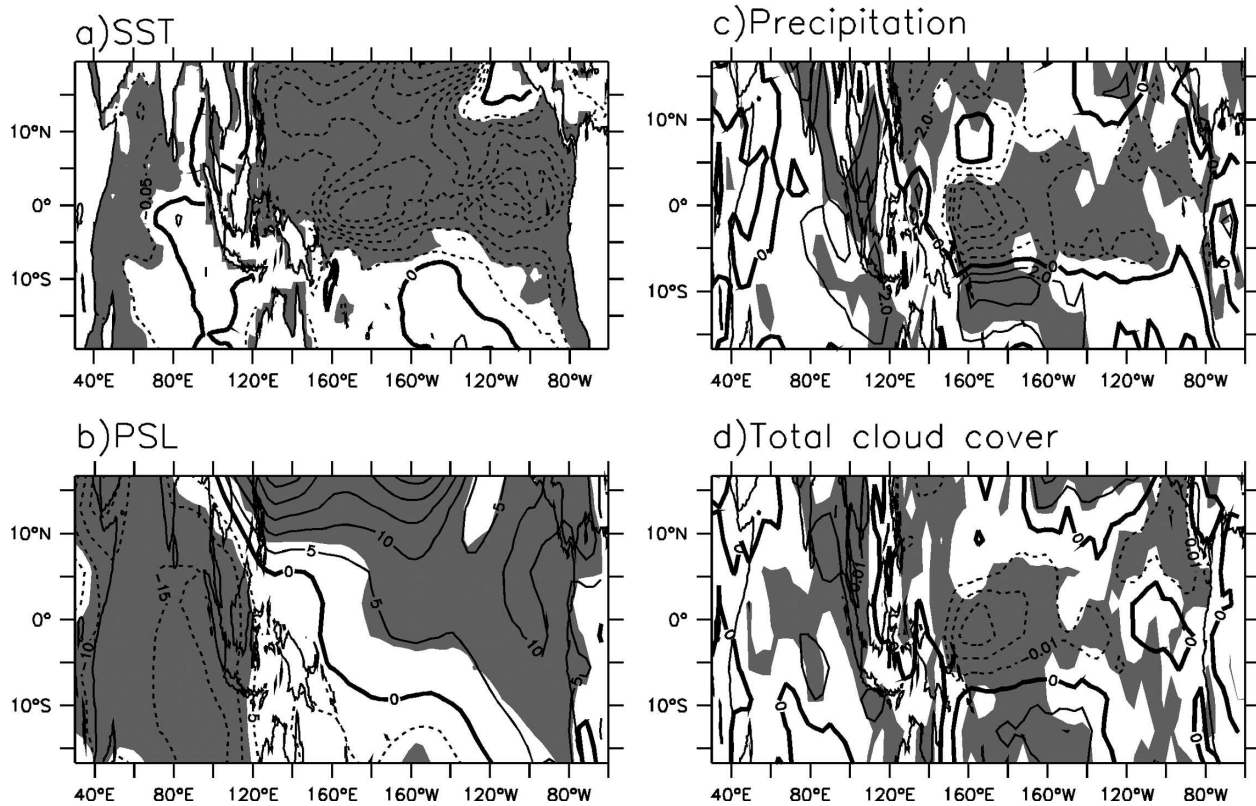


FIG. 4. Regression of tropical (a) SST ($CI = 0.05^{\circ}\text{C}$), (b) PSL ($CI = 5\text{ Pa}$), (c) precipitation ($CI = 2 \times 10^{-9}\text{ m s}^{-1}$), and (d) total cloud cover ($CI = 0.01$ fraction) in CTRL onto the multidecadal index defined in Fig. 3. All data are bandpass filtered to retain variability at a 20–80-yr time scale. Shading indicates regressions significant at the 90% confidence level.

How is the tropical multidecadal variability involved in such tropical–extratropical linkage? The EOF modes of tropical multidecadal variability are obtained through the same procedures as for the North Pacific multidecadal SST mode. All tropical climate variables were low-pass filtered before EOF analysis. These newly derived EOF modes (not shown) are very similar to those North Pacific associated patterns discussed above (Fig. 4); the temporal evolution of these tropical modes corresponds well to the multidecadal index at time scales longer than 20 yr. All the projection time series associated with tropical EOF modes (Figs. 5b–e) are significantly correlated with the multidecadal index (Fig. 5a) at a range of 0.64–0.74, with correlations maximized at 0 lag. Such correspondence is confirmed by coherence analysis of these tropical time series and multidecadal index without low-pass filtering; all coherence spectra (Figs. 5f–i) exhibit statistically significant squared coherence (~ 0.5) on a quasi-50-yr frequency band. Therefore, both the North Pacific associated patterns and the tropical EOF patterns depict virtually the

same multidecadal mode in the tropical climate system, which is closely connected to the extratropical multidecadal variability. This implies that multidecadal variability in the tropics is dominated by that associated with the North Pacific variability. It is worth mentioning that the results of Fig. 5 are basically reproducible using the leading principal components of unfiltered extratropical SLP and tropical fields. That is to say, the multidecadal linkage is not simply an artifact of a low-pass filter, but a real feature in CTRL.

With the establishment of a multidecadal tropical–extratropical linkage, its cause needs to be identified. Does it originate from the tropics, as envisaged by numerous observational studies (Zhang et al. 1997; Minobe 1997; Deser et al. 2004), or from the extratropics as suggested by Barnett et al. (1999) and Vimont et al. (2001)?

The statistical model of Newman et al. (2003) has been invoked to assess a tropical-induced tropical–extratropical linkage. In agreement with the observation, all of the multidecadal variability in the North

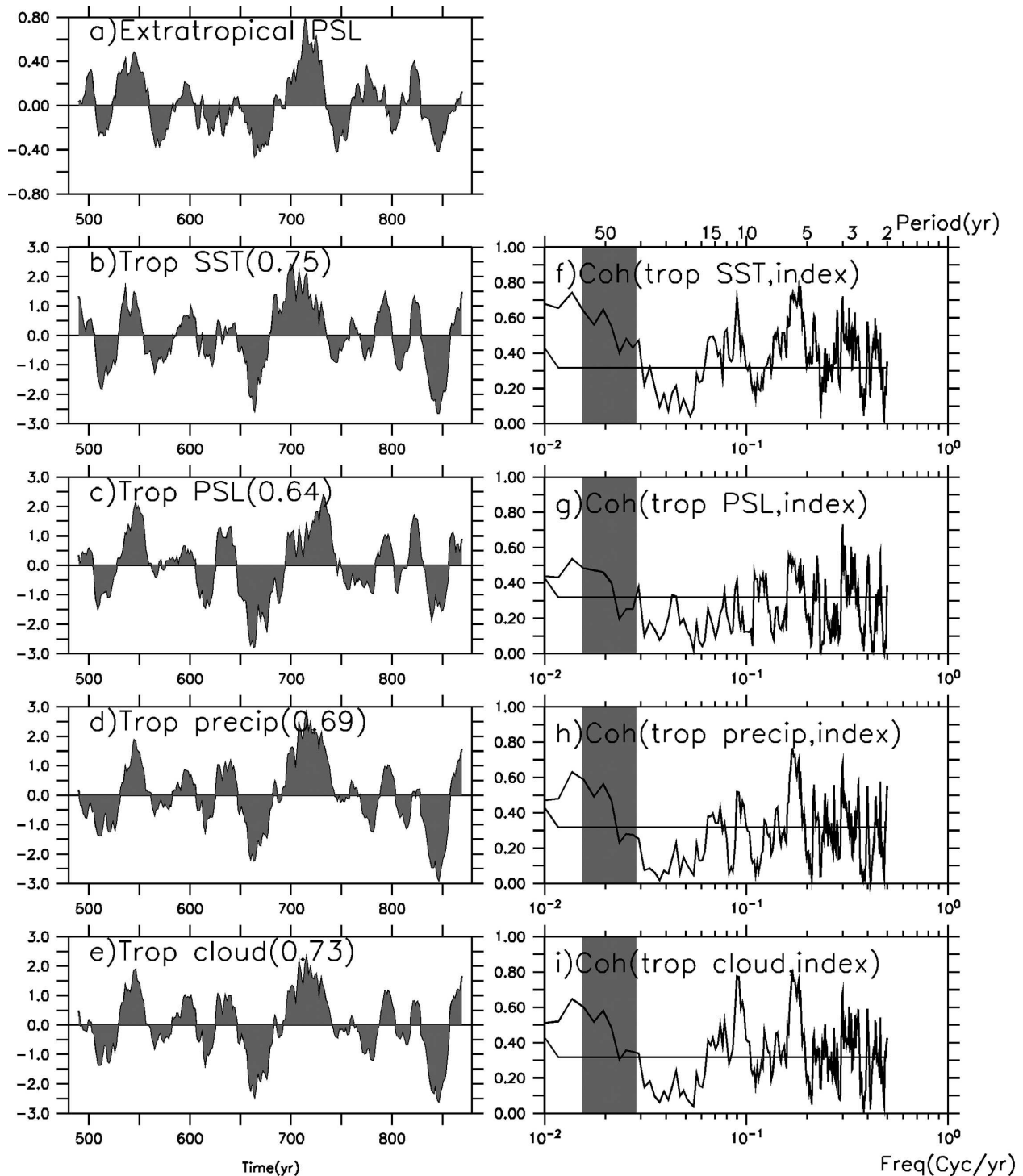


FIG. 5. (a) The multidecadal index with 20-yr low-pass filtering. (b)–(e) The 20-yr low-pass-filtered time coefficients (normalized) of leading EOFs of tropical multidecadal variability in CTRL. Prior to EOF analyses, tropical datasets are low-pass filtered to retain the variability longer than 20 yr. Time coefficients are then obtained by projecting unfiltered data onto leading EOF patterns. Values in parentheses are correlation coefficients between these low-pass-filtered tropical time series and multidecadal index as shown here. (f)–(i) Coherence spectra of the unfiltered tropical time series and multidecadal index. The 90% confidence level is indicated. The quasi-50-yr frequency band is highlighted with shading.

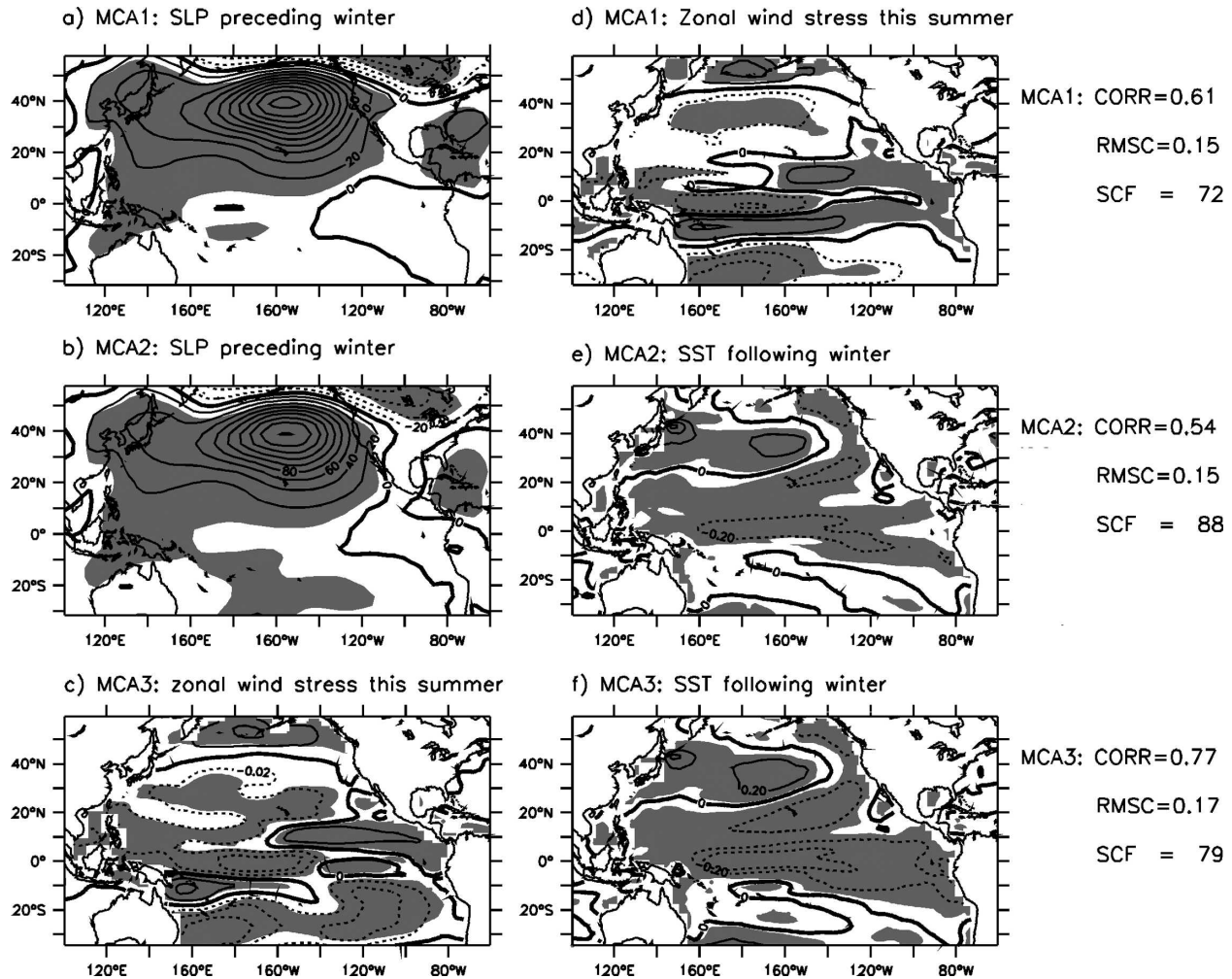


FIG. 6. Leading heterogeneous patterns resulting from MCA analyses of (a), (d) SLP in the preceding winter and zonal wind stress this summer for MCA1; (b), (e) SLP in the preceding winter and SST in the following winter for MCA2; (c), (f) zonal wind stress this summer and SST in the following winter for MCA3. Units are 20 Pa for SLP, 0.02 dyn cm^{-2} for zonal wind stress, and 0.2°C for SST. The shading indicates regressions significant at the 90% confidence level. Standard statistics of MCA given are the correlation (CORR) between the two resulting time series, the normalized RMSC, and the SCF explained by the leading mode.

Pacific SST in CTRL appears attributable to the reddening processes of tropical teleconnective and extratropical local forcing, according to the argument of Newman et al. (2003). Unlike in the observation though, the North Pacific SST variability in CTRL is more a reddening process of extratropical local forcing than reddening of tropical teleconnective forcing, which is a model deficiency common to many GCMs as pointed out by Newman (2007).

Intricately, an extratropical origin is also possible for the modeled multidecadal linkage, since the SFM can be shown to operate in CTRL. Following Vimont et al. (2003), the relationship between winter (November–March) extratropical SLP, summer (April–August) northern tropical zonal wind stress, and winter (Octo-

ber–February) tropical SST is examined with maximum covariance analysis (MCA; Bretherton et al. 1992). The procedures of data processing have been exactly followed: the data domain and time interval averaged were identical, ENSO influence was linearly removed, and the unfiltered data were detrended and standardized before MCA. A detailed description of the data processing can be found in section 2 of Vimont et al. (2003). The leading pairs of heterogeneous regression maps resulting from the MCA are presented in Fig. 6 in similar fashion as Vimont et al.'s (2003) Fig. 3. The standard statistics of MCA are given as well, including the correlation (CORR) between the two resulting time series, the normalized root-mean-squared covariance (RMSC), and the squared covariance fraction (SCF)

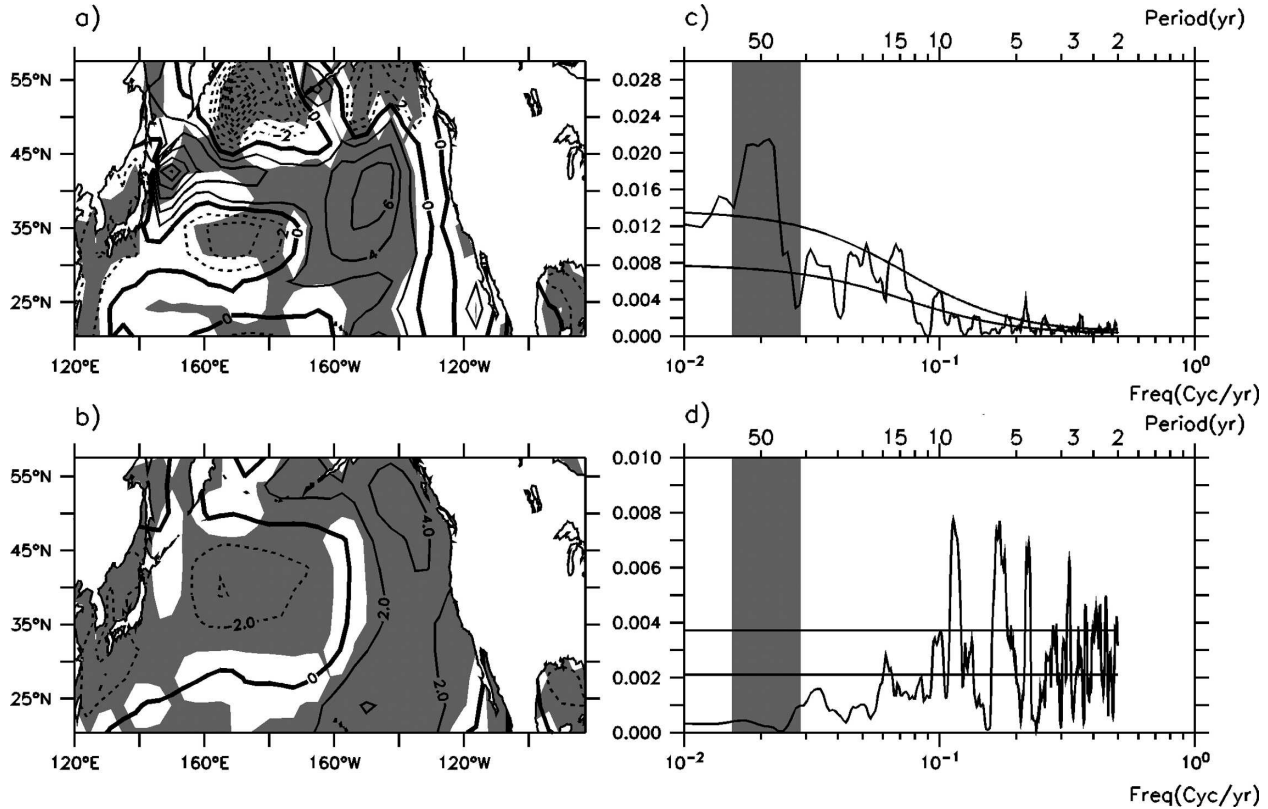


FIG. 7. (a) Same as in Fig. 4, but for North Pacific turbulent heat flux in CTRL. Upward heat flux is defined as positive. $CI = 2 \text{ W m}^{-2}$. (b) Same as in (a), but for regression at high-frequency band. All data are 7-yr high-pass filtered. (c), (d) Power spectrum of the projected time series (normalized) associated with the heat flux regression pattern in (a) and (b), respectively. The 90% and 50% confidence levels are indicated. The quasi-50-yr frequency band is highlighted with shading.

explained by the leading mode. All the statistics indicate the three fields are strongly coupled. Figure 6 may be summarized as follows. The extratropical SLP variability in winter leads to zonal wind stress anomalies that extend onto and south of the equator in the following summer; these zonal wind stress anomalies, in turn, excite equatorial SST variability in the next winter. Capturing the overall picture of SFM, Fig. 6 shows a fundamental discrepancy from the observational counterpart. It is essentially the NAM playing in the modeled SFM (Figs. 6a,b); in reality, the responsible extratropical SLP variability has a spatial structure of the so-called North Pacific Oscillation (NPO; Rogers 1981). Nevertheless, the results of Fig. 6 indicate the SFM is operative in CTRL. In principle, the SFM operates at all time scales and may be responsible for the modeled tropical–extratropical linkage. To confirm this, coherence/cross-spectrum analysis has been done for all the three pairs of time series resultant from the MCA analysis. Strong multidecadal coherence is found between each pair of the MCA time series at near-zero phase lag. Moreover, all in-phase cospectra of the three

pairs of MCA time series share the quasi-50-yr peak (not shown), indicating the influence of the extratropical multidecadal variability onto the tropics via the SFM. Therefore, the role of the tropics in the PMV cannot be clarified with statistical assessment alone.

b. Midlatitude air–sea interaction

Midlatitude air–sea interaction acts as another candidate for the genesis of atmospheric multidecadal variability. A hint of midlatitude oceanic feedback to the atmosphere is the turbulent heat flux forcing of the atmosphere by the upper ocean at multidecadal time scale. The pattern of the North Pacific heat flux (Fig. 7a) associated with the PMV largely resembles the underlying SST pattern (i.e., multidecadal SST mode in Fig. 2a), with upward heat flux over the warm SST anomalies in the KOE and CNP regions; the quasi-50-yr peak in the power spectrum of the projection time series of the heat flux pattern (Fig. 7c) substantiates a multidecadal forcing of the atmosphere by midlatitude ocean. Similar results are obtained based on different model simulations (Pierce et al. 2001; Kwon and Deser

2007). A consistent atmospheric response to such oceanic forcing, however, is not ensured, because of the energetic internal atmospheric variability in extratropics. The heat flux association at an interannual time scale is distinct from the above at multidecadal scale. At interannual scale, the projection of heat flux onto the multidecadal SLP index yields downward heat flux over warm SST in the western and central North Pacific (Fig. 7b), in line with the notion that turbulent heat flux associated with the atmospheric bridge acts as the driving force on midlatitude SST in ENSO scenarios (Alexander et al. 2002). The power spectrum of the projection time series associated with the interannual heat flux pattern confirms such heat flux forcing on the ocean is limited to short time scales within a decade (Fig. 7d).

Another indication of atmospheric response to ocean is the quasi-50-yr peak in the NH atmospheric SLP (Fig. 3), which suggests that the atmosphere is involved in the PMV. However, it remains unclear from the control experiment whether the atmosphere responds to the tropical or extratropical SST.

The statistical analyses above have identified important features of the PMV. Yet none of these analyses are conclusive in determining the origin of PMV. Neither the tropical nor the extratropical origin can be excluded. Both tropical forcing and midlatitude oceanic feedback could still be responsible for the multidecadal atmospheric variability. To clearly identify the origin of the PMV in CTRL, sensitivity experiments are performed as discussed below.

5. The origin of PMV: Inference from sensitivity experiments

Two sensitivity experiments are designed specifically for the identification of the origin of PMV. The modeling strategy used is “partial coupling,” which was outlined in section 2. Experiment PC-ET is used to simulate a climate system without the tropical-driven atmospheric bridge. With application of the PC approach to tropical regions within 20° , the ocean and atmosphere are decoupled in the tropics. The tropics now play a passive role in the global climate system, because of the loss of energetic coupled variability and the resultant teleconnect through the atmospheric bridge. Under such circumstances, the extratropics retains full atmosphere–ocean coupling in the absence of perturbation from the tropical climate variability. If the extratropical atmosphere still exhibits preferred multidecadal variability, it cannot be attributed to tropical coupled variability. In contrast, experiment PC-T retains full coupling in the tropics and precludes any direct oceanic

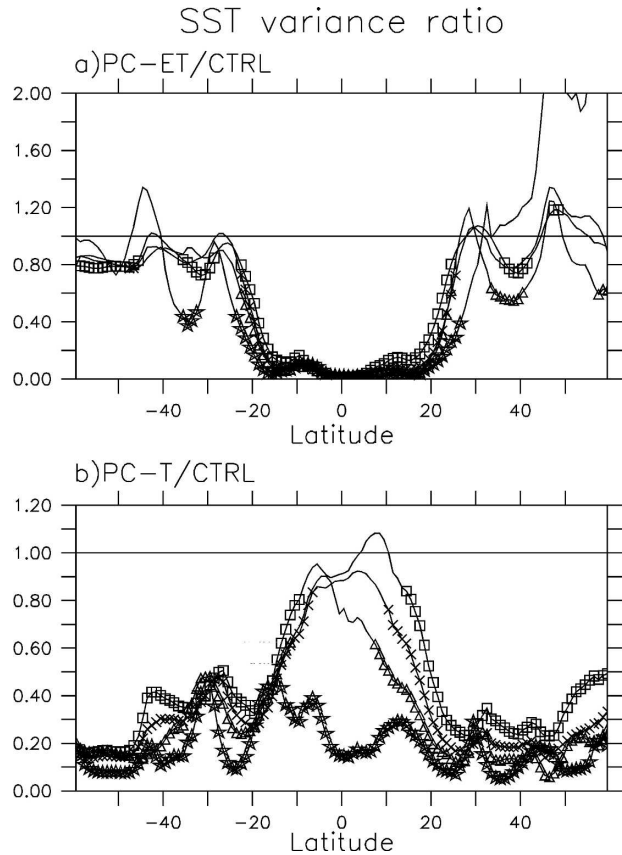


FIG. 8. Zonal means of the Pacific SST variance ratio between (a) PC-ET and CTRL and (b) PC-T and CTRL at 20–80-yr (star), 7–20-yr (triangle), 1–5-yr (square), and all (cross) time scales. Symbols are marked where the values are significant at the 90% confidence level with the two-tail F test.

feedback to the atmosphere in the extratropics outside of 20° . With regard to midlatitude SST, such a setting can be viewed as the statistical model of Newman et al. (2003), except for the inclusion of active oceanic dynamics. If preference for multidecadal variability is found in extratropical atmosphere in PC-T, it can be ascribed to a tropical–extratropical or intrinsic tropical origin.

Outputs from experiments PC-ET and PC-T are analyzed similarly as the CTRL. Figure 8 shows the zonal means of the Pacific SST variance ratio between sensitivity experiments and CTRL in several frequency bands. Without tropical air–sea interaction in PC-ET (Fig. 8a), SST variability is virtually suppressed in the tropical Pacific, as expected. There appears to be substantial variance reduction in the midlatitudes of both hemispheres at interannual (<5 yr) and decadal (7–20 yr) time scales, which can be attributed to the teleconnective impact of tropical Pacific climate variability; the tropical influence on North Pacific multidecadal SST variance, however, is not significant at 90% confidence

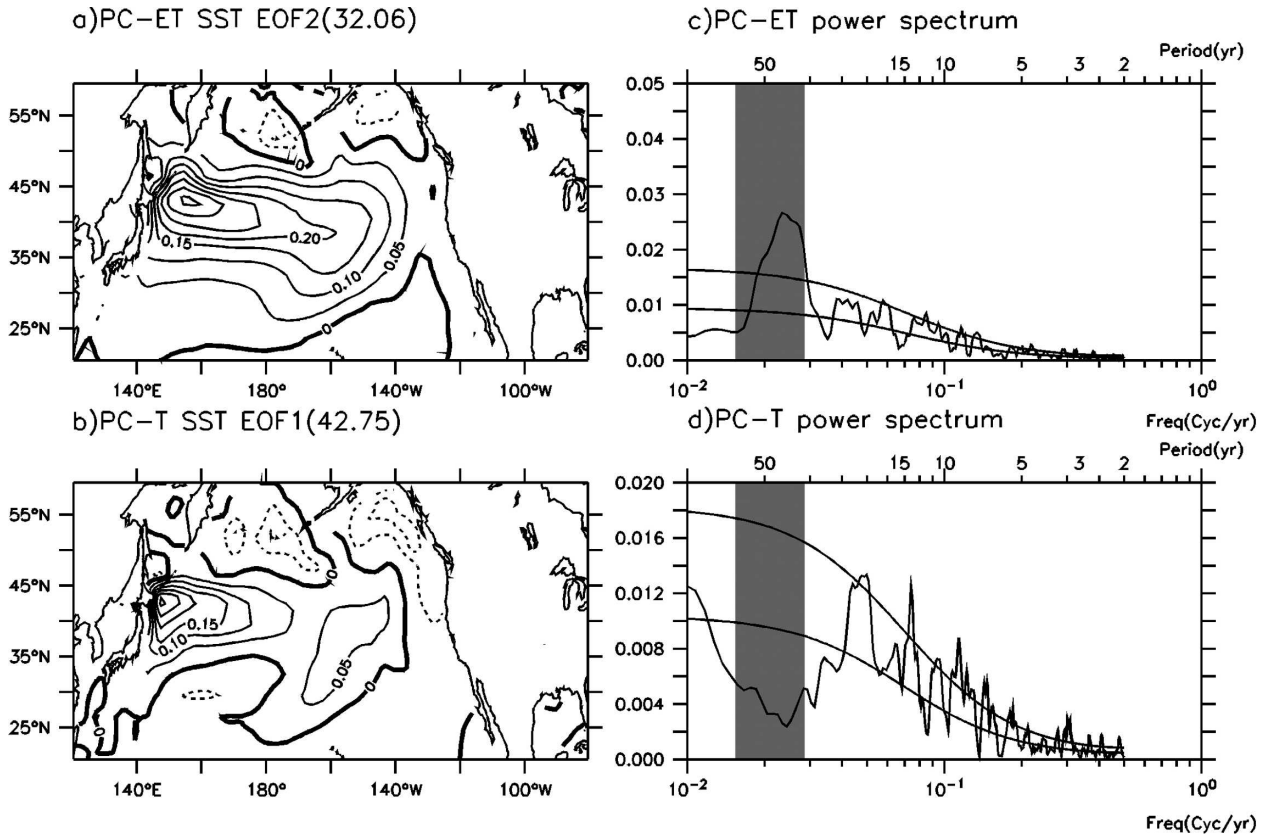


FIG. 9. (a), (c) Same as in Fig. 2, but for experiment PC-ET. (b), (d) Same as in Fig. 2, but for PC-T.

level with the two-tail F test, though this result is somewhat sensitive to the choice of frequency cutoff. In contrast to PC-ET, PC-T (Fig. 8b) exhibits much weaker (<50%) signals in the extratropics at all frequency bands, because of a restoring damping effect on SST that is inherent to the PC surgery.

Most interesting here is the dramatically reduced tropical multidecadal SST variability in PC-T compared to CTRL. The original variability is reduced by 80% with the decoupling of air–sea interaction in the extratropics in PC-T. This is in sharp contrast to the insignificant impact on other frequency bands, suggesting the negligible effect of the extratropics on the intensity of tropical variability at decadal and interannual bands. At the interannual band, this negligible effect from the North Pacific is easy to understand: tropical interannual variability is dominated by ENSO, which originates from the tropics. The negligible impact on the tropical decadal variability suggests that this variability is likely to originate locally from the tropics. In comparison, the multidecadal variability originates from the North Pacific. This conclusion is largely consistent with the results of L02 and W03 in another coupled GCM—FOAM.

Combining with the statistical assessment in last section, the experiment results suggest tropical multidecadal variability in CTRL arises from the North Pacific through the teleconnect mechanism of SFM. Its existence critically depends on the multidecadal variability in the extratropics and the air–sea coupled conduit of SFM. As suggested by Wu et al. (2007), the coupled wind–evaporative–SST (WES) feedback (Liu and Xie 1994) is assumed to play a crucial role in the teleconnect mechanism of SFM. Once the extratropics loses most of its multidecadal variability, or tropical air–sea interaction is forbidden, the tropical multidecadal signals virtually disappear as in PC-T and PC-ET, respectively. The tropical multidecadal variability, however, may serve as a potential positive feedback to the original extratropical variability (Wu et al. 2007).

How does the extratropical multidecadal mode react to the suppression of air–sea interaction? In PC-ET, the PMV mode of PDO-like structure (Fig. 9a) appears as the second leading mode of extratropical SST variability, accounting for 32% of the total multidecadal variance, compared to 48% in CTRL. Unlike the relatively even loading between KOE and CNP in CCSM3 (Fig. 2b), this PC-ET mode exhibits intensified variability

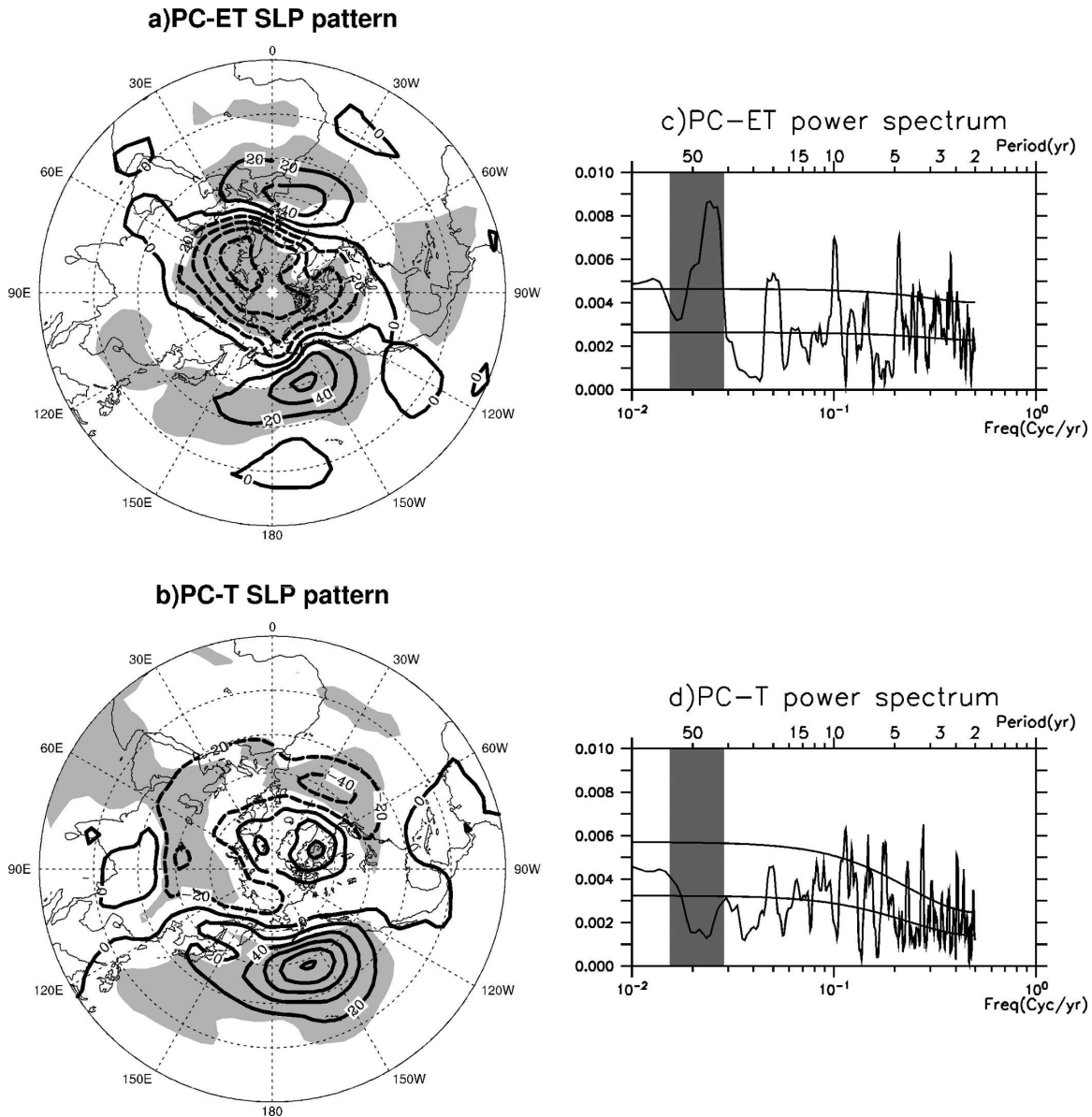


FIG. 10. (a), (c) Same as in Fig. 3, but for experiment PC-ET. (b), (d) Same as in Fig. 3, but for PC-T.

toward the western boundary along 40°N . Both the downscaling and variability reloading are likely attributed, partly, to the absence of tropical positive feedback, since the tropical teleconnective impact is stronger on the central and eastern North Pacific (Deser and Blackmon 1995; Alexander et al. 2002). The temporal evolution of this PMV mode in PC-ET is characterized by a quasi-50-yr peak as seen in the power spectrum of Fig. 9c, similar to that in CTRL.

In the extratropical atmosphere, the largely NAM-like pattern (Fig. 10a versus Fig. 3a) and its characteristic multidecadal time scale (Fig. 10c versus Fig. 3b) are retained in PC-ET; subtle changes are found in the

orientation of the atmospheric flow over the western North Pacific, which, again, may be related to the tropical feedback. Collectively, the favorable comparison between the PMV in PC-ET and CTRL leads us to conclude that the PMV originates internally from the extratropical coupled climate system, rather than the tropical coupled variability.

Analysis of the multidecadal mode in PC-T confirms the midlatitude origin of PMV. The leading mode of North Pacific SST explains 43% of the total multidecadal variance (Fig. 9b). The power spectrum of the projection time series associated with this SST mode (Fig. 9d) is characterized by a deficit of multidecadal power

relative to adjacent frequency bands. The associated atmospheric SLP (Fig. 10b) is also changed, exhibiting a local high pressure system rather than the NAM-like teleconnective structure as in CTRL and PC-ET; its temporal evolution (Fig. 10d) lacks multidecadal variability, consistent with the underlying SST. Consequently, the previous conclusion is reinforced: a majority of PMV in CTRL is not generated by tropical coupled variability, but is a phenomenon inherent to extratropical climate system.

Given that the PMV is of intrinsic midlatitude origin, the multidecadal variability in the extratropical SLP field (Fig. 3b) and oceanic heat flux forcing (Fig. 7c) signifies a coupled midlatitude origin that is characterized by a large-scale air–sea interaction at midlatitudes. The quasi-50-yr peak in the SLP in PC-ET (Fig. 10b) further suggests that the atmospheric response to the North Pacific Ocean, as well as the ocean–atmosphere coupling over the North Pacific, plays an active role in the formation of the PMV mode. The importance of the atmospheric response to North Pacific oceanic variability on the PMV is consistent with the recent studies on the atmospheric response (Liu and Wu 2004; Liu et al. 2007). The detailed mechanism underlying the PMV, however, is still in progress.

6. Discussions

Here, we further discuss several issues related to the PMV.

a. Basin-scale versus local atmospheric forcing

Recently, Latif (2006) suggests that the PMV in their coupled GCM is caused by spatial resonance. He bases his conclusion on the lack of significant spectral peak in local wind stress. We caution about this conclusion. Instead, we point out that the PMV is associated preferentially with large-scale atmospheric variability rather than local wind. Physically, low-frequency variability in the ocean, whose long-term memory resides in the slow gyre circulation adjustment in the form of westward-propagating Rossby waves, is driven by large-scale wind stress curl, instead of small-scale local wind stress (Latif and Barnett 1994; Frankignoul et al. 1997; Jin 1997). In the framework of a reduced gravity model, the baroclinic ocean response is governed by

$$\frac{\partial h}{\partial t} - c \frac{\partial h}{\partial x} = -\mathbf{k} \cdot \nabla \times \boldsymbol{\tau} / \rho_o f_o, \quad (1)$$

where h is thermocline depth, $\nabla \times \boldsymbol{\tau}$ is wind stress curl forcing, c is the Rossby wave speed, ρ_o is seawater den-

sity, and f_o is the Coriolis parameter at the reference latitude. The boundary condition at the eastern boundary x_E can be reasonably assumed to be $h(x_E, t) = 0$ (Schneider et al. 2002; Kwon and Deser 2007). The solution for h ,

$$h(x, t) = \frac{1}{\rho_o f_o} \int_{x_E}^x \mathbf{k} \cdot \nabla \times \boldsymbol{\tau} \left(x', t - \frac{x' - x}{c_o} \right) dx', \quad (2)$$

shows that the response at a particular longitude is determined by the integrated effect to the east; that is, nonlocal forcing plays an important or even dominant role. Obviously, ocean response to wind stress curl forcing of larger spatial scale is selectively enhanced due to the coherent accumulation along with the Rossby wave propagation. In the meantime, wind stress anomalies of small spatial scales do not contribute to the integral, and therefore do not contribute to the PMV significantly.

The nature of active large-scale ocean–atmosphere coupling for the PMV is identified in the large-scale wind field, but not necessarily in the local wind. The wind stress curl forcing associated with the PMV mode in CTRL (Fig. 11a) and PC-ET (not shown) is of basin scale, with anticyclonic anomalies predominant over the North Pacific spanning across 160°E–140°W. A quasi-50-yr peak is evident in the power spectrum of its associated time series (Fig. 11b). In contrast, such preferred multidecadal variability does not exist in the local wind stress forcing. For example, the spectra of wind stress curl over the activity center of the regression pattern (45°N, 160°W in Fig. 11a) and that in the northwestern Pacific (40°N, 160°E in Fig. 2a; where SST signal is heavily loaded) show no distinguished multidecadal spectral peak beyond white noise background (Fig. 11c), which is consistent with the findings of Latif (2006).

b. Latif–Barnett feedback mechanism

As Schneider et al. (2002) pointed out, some features of the genesis of North Pacific climate variability can be inferred from the lead–lag relationship between CNP and KOE signals. For example, the CNP signal is expected to follow that of the KOE region in the scenario of coupled midlatitude origin as the Latif–Barnett mechanism, with the CNP ocean responding passively to overlying atmospheric anomalies that are affected by KOE conditions. Alternatively, a positive correlation at CNP SST anomalies leading those in the KOE region by several years, resultant from the westward propagation of Rossby waves, may imply other origins of decadal variability in the Pacific as described in the intro-

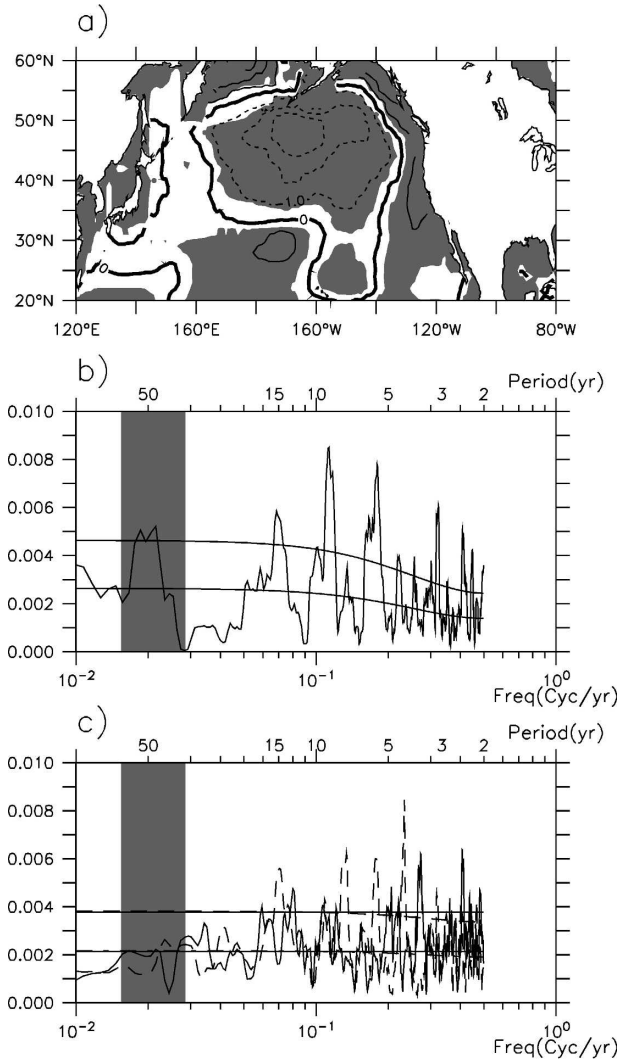


FIG. 11. (a) Same as in Fig. 4, but for the North Pacific wind stress curl in CTRL. $CI = 1.0 \times 10^{-8} \text{ Pa m}^{-1}$. (b) Power spectrum of the projected time series (normalized) associated with this wind stress curl regression pattern. (c) Power spectra of wind stress curl over the activity center of the regression pattern (45°N , 160°W ; solid) and that in the northwestern Pacific (40°N , 160°E ; dashed). The 90% and 50% confidence levels are indicated. The quasi-50-yr frequency band is highlighted with shading.

duction. In observation, maximum positive correlation is found at CNP leading KOE SST by 5 yr (Seager et al. 2001; Schneider et al. 2002). Such a lead-lag relationship seems to be absent in CCSM3. The correlations between KOE SST and CNP quantities are calculated in CTRL and PC-ET. Clearly, warm (cool) SST anomalies develop in CNP (Fig. 12a, the reason why SST lags local forcing has been illustrated in the last subsection) and KOE (Fig. 12b) regions a few years later than the formation of anticyclonic (cyclonic) wind stress curl in CNP, and subsequently exert a cyclonic (anticyclonic)

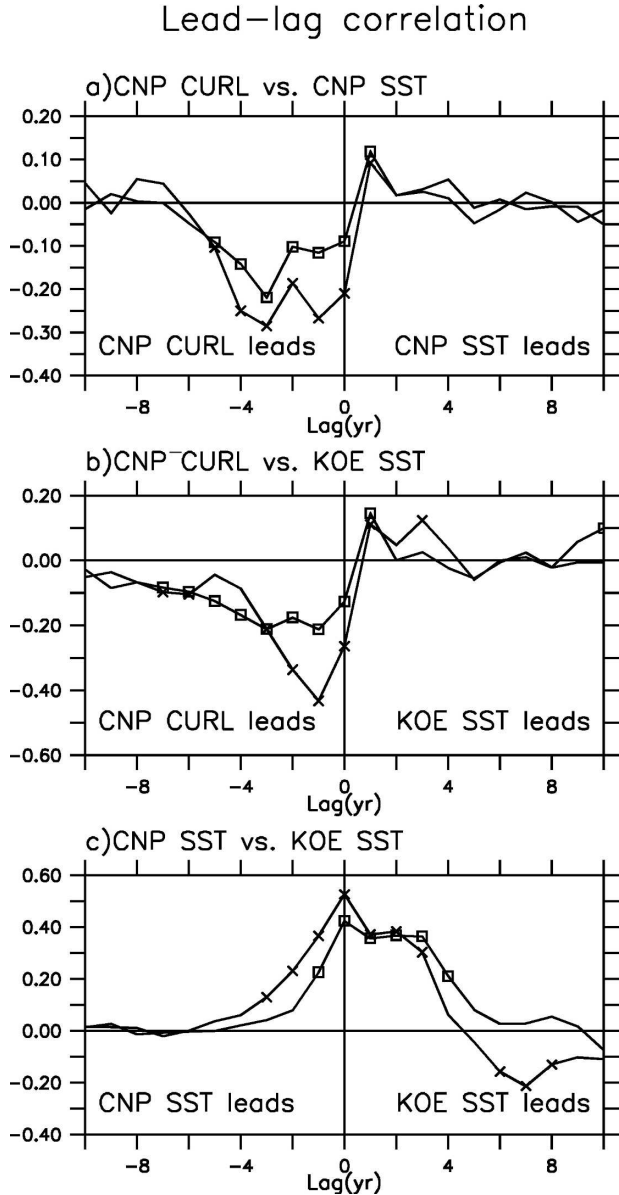


FIG. 12. Lead-lag correlation between (a) CNP wind stress curl and CNP SST, (b) CNP wind stress curl and KOE SST, and (c) CNP SST and KOE SST in CTRL (cross) and PC-ET (square). Symbols are marked where the values are significant at the 90% confidence level with the two-tail t test.

perturbation back to the CNP wind stress curl field. Meanwhile, slight asymmetry of lead-lag correlations between KOE and CNP SST (Fig. 12c) indicates a more significant influence on CNP by KOE anomalies than vice versa, which may be due to the mean eastward advection by the KOE.

Collectively, CCSM3 results represent a relatively more interactive relationship between CNP and KOE signals: the forcing of CNP wind stress curl incites like-

Associated extratropical patterns

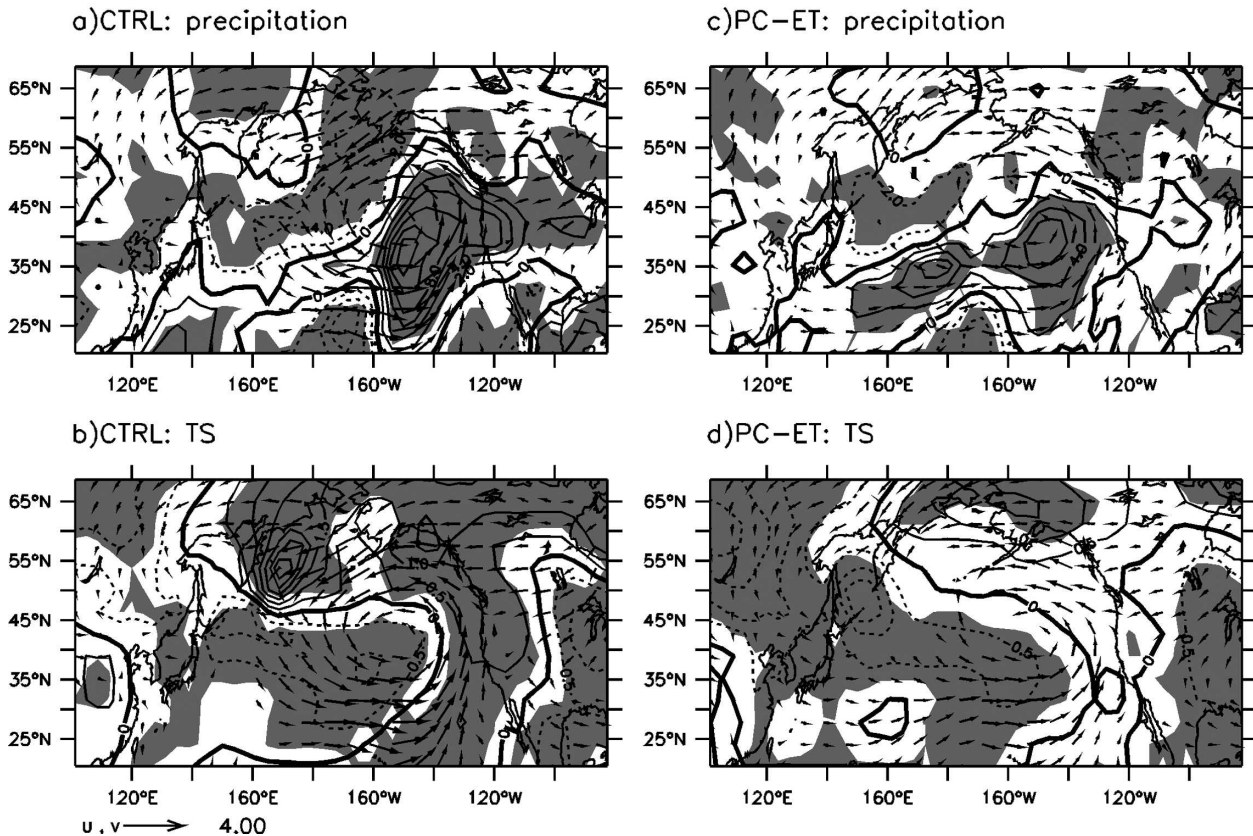


FIG. 13. (a), (b) Same as in Fig. 4, but for North Pacific precipitation ($CI = 2 \times 10^{-9} \text{ m s}^{-1}$) and surface air temperature ($CI = 0.5^\circ\text{C}$) during wintertime (December–January) in CTRL. (c), (d) Same as (a), (b), but for PC-ET. Vector represents the associated wind field at 1000 hPa that is significant at the 90% confidence level. Unit length stands for a wind anomaly of 4 m s^{-1} .

sign SST anomalies in the CNP first and the KOE a few years later (up to 7 yr in Fig. 12b), in agreement with the observation; subsequently, KOE returns information via both atmosphere and oceanic routes, with the latter dominating the CNP SST changes. While the information return from KOE is uncertain in observation, a hint has been given by Nakamura et al. (1997) that the cooling in CNP was predated by cooling in KOE 2 yr before during the 1976/77 shift. Nevertheless, an oceanic feedback to extratropical atmosphere clearly exists in the CCSM3 model system, in favor of a coupled midlatitude origin of PMV in CCSM3.

c. Impact on midlatitude climate

An inspection of associated patterns of the midlatitude atmospheric fields unveils significant climate impact from the PMV in CCSM3. Figure 13 gives the spatial distribution of wintertime (December–February) air surface temperature and precipitation anomalies during the persistence of an abnormally

strong Aleutian low. The annual mean patterns are basically identical, though 75% weaker. The choice of wintertime results shown here is for direct comparison with the observation (Deser et al. 2004). The changes agree well with the anomalous atmospheric circulation: anomalous northerly flow over the western-central North Pacific reduces the moisture flux into coastal Asia, leading to dryness and lowering surface air temperature there; to the east, anomalous southerly flow brings more moisture from warm ocean and results in higher winter temperatures and ample precipitation along the west coast of United States; under the prevailing of easterly anomalies, Alaska and western Canada undergo warmer winters without much precipitation. In comparison to the observed climate impact (Cayan et al. 2001; Deser et al. 2004), the model shows a substantial discrepancy: the banded structure of precipitation conditions over North America exhibits the opposite sign to historical record. This discrepancy may be related to the different orientation of the simulated

atmospheric circulation, particularly over the eastern basin of North Pacific and North America.

Interestingly, PC-ET demonstrates overall similar climate impacts to those of CTRL, which suggests that the extratropical multidecadal variability can directly affect the climate conditions over the neighboring land areas without the mediation of the tropics, at least in CCSM3. Therefore, long-term predictions of climate conditions over land areas, including North America and eastern Eurasia, require knowledge of multidecadal variations in the North Pacific region, which may potentially be predictable (Pierce et al. 2001).

d. The role of ENSO

What is the role of ENSO variability in the PMV? A comparison of ENSO (not shown) and multidecadal EOF patterns of multiple tropical fields reveals a broad similarity of tropical variations at interannual and multidecadal time scales. An apparent difference, though, is the more equal weighting spreading over the tropical Indo-Pacific for the multidecadal patterns, which is common to all the climate fields inspected, including SST, SLP, precipitation, and total cloud cover. Such a feature agrees well with the observational findings of Garreaud and Battisti (1999). When analyses of Fig. 5 are repeated with these newly derived tropical principal components in replacement of the associated multidecadal time series, good correspondence remains between the extratropics and tropics at multidecadal time scale. Thus, the implication is that the multidecadal variability in the North Pacific excites corresponding variations in the tropics, which in turn act as a fluctuant background for the ENSO variability (Fedorov and Philander 2000; Yang et al. 2005; Zhang et al. 2005).

e. Is the PMV merely sampling error?

The short duration of historical datasets poses huge challenges to the study of multidecadal climate variability. The potential multidecadal variability identified in the observational NPI could be regarded as multidecadal components of a pure stochastic process internal to the extratropical atmosphere, which is prevalent during the twentieth century only incidentally. Such “preferred” multidecadal variations, in turn, induce coherent responses in the underlying ocean (Hasselmann 1976). In other words, covarying atmospheric and oceanic variability of multidecadal preference may simply be a sampling error easily arising from infinite sampling. This has been demonstrated to account for an outstanding 20-yr North Pacific mode in a coupled model simulation (Schneider et al. 2002).

Such a sampling error is less likely to be the cause of

PMV in CCSM3. First, both CCSM3 control integration and experiment PC-ET exhibit the same quasi-50-yr multidecadal peak, which is very unlikely to be a coincidence. Instead, this robust feature suggests this PMV mode is inherent to the model climate system. Second, a pronounced multidecadal heat flux forcing on atmosphere is observable in CTRL (Fig. 7) and PC-ET, suggesting a plausible source for the multidecadal variability of extratropical atmospheric circulation. It should also be pointed out that the North Pacific origin of the PMV is consistent with the previous study in the independent climate model FOAM (L02 and W03).

Whether the real atmospheric multidecadal variability of the NH extratropics stands for a pure stochastic process, or as a response to heat flux forcing by the upper ocean, is still an open question. The atmospheric response to North Pacific oceanic forcing at seasonal time scale has been intensively studied during the last decade (Peng et al. 1997; Kushnir et al. 2002). There appears to be a consensus on a modest magnitude of atmospheric response, irrespective of its structure and polarity. Things can be different at longer time scales, though (Rodwell et al. 1999; Czaja and Marshall 2000). A recent study by Liu et al. (2007) shed some light on the atmospheric response to longer-time-scale oceanic variability. It shows that the atmospheric response becomes more significant at annual and longer time scales, because of the rapid increasing of the signal-to-noise ratio with time scale. Indeed, atmospheric response at longer time scales is more relevant to climate variability of decadal and longer time scales. Further effort is needed to understand the origin of atmospheric multidecadal variability in the observation.

f. Centennial-scale modulation of the PMV

An interesting feature of the PMV revealed by recent studies (D'Arrigo et al. 2005; Latif 2006) is the substantial centennial-scale modulation that is perceptible in multicentury-long time series. Such a modulation is indicated by the CCSM3 simulation. Figure 14 displays wavelet power spectrum of the time series associated with the multidecadal SST mode in CTRL (Torrence and Compo 1998). The quasi-50-yr period signal identified by multitaper spectrum analysis (Fig. 2b) is confirmed by wavelet analysis (Fig. 14b). This multidecadal signal undergoes centennial-scale modulation, characterized by active periods of model years 480–650 and 730–880, and the quiescent period in between (Fig. 14a). The cause of the centennial-scale modulation, however, is an open question. Longer time series will be needed to address this question, as pointed out by Latif (2006).

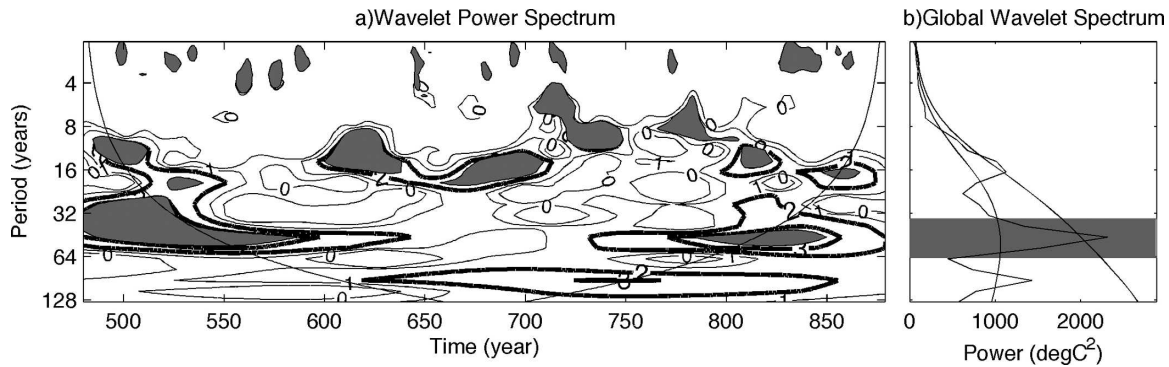


FIG. 14. (a) Wavelet power spectrum and (b) global wavelet spectrum of the projection time series associated with the multidecadal SST mode in Fig. 2 for CTRL. For (a), contours correspond to \log_2 (power); values larger than 2 are emphasized in thick lines and those less than zero are omitted for clarity. Shading denotes power significant at the 90% confidence level, and anything beyond the cone of influence is dubious. For (b), the 90% and 50% confidence levels are indicated. The quasi-50-yr frequency band is highlighted with shading.

7. Summary

The origin and nature of the PMV in CCSM3 is investigated with a combination of statistical and dynamical approaches. The CTRL simulates a PMV with expressions in both ocean and atmosphere, similar to the observation. Differing from the real PMV, however, the atmospheric pattern of the modeled PMV resembles the NAM rather than the PNA.

To examine the role of the tropics in the PMV, a multidecadal tropical–extratropical linkage has been established as a robust feature in CTRL following Deser et al. (2004). The origin of this linkage is then assessed statistically with CTRL output. While confirming the two-way tropical–extratropical interactions, such a statistical assessment, however, cannot exclusively identify the origin of the modeled multidecadal linkage. The origin of the PMV therefore remains elusive.

Sensitivity experiments are performed to investigate further the origin of PMV. With the atmosphere decoupled from the tropical ocean in PC-ET, the NH extratropical climate system retains its capability of creating pronounced multidecadal variability, yet fails to produce coherent responses in the tropics as in CTRL. By contrast, experiment PC-T is set up with atmosphere–ocean decoupled in the extratropics. Based on PC-T results, the tropical coupled variability can be excused from the genesis of PMV, because the multidecadal variability is virtually suppressed in the tropics as well as in the extratropical atmospheric and SST fields.

The picture of PMV in CTRL can be described as follows. An intrinsic midlatitude coupled origin gives rise to multidecadal variability in the North Pacific re-

gion; this extratropical signal then imprints itself in the tropical Indo-Pacific in the carriage of SFM, while establishing a robust tropical–extratropical linkage. Similar extratropical control of tropical climate at decadal and longer time scales has been suggested to be operative in another coupled GCM—FOAM (Wu et al. 2007).

The PMV has been reported to arise from the multidecadal variability in the North Atlantic thermohaline circulation (Timmermann et al. 1998). However, such a possibility of Atlantic-originated PMV has been excluded through careful examination of both CTRL and PC-ET outputs, as well as further performance of sensitivity experiment. The leading evidence are listed as follows. First, the quasi-50-yr peak is not evident in the power spectrum of the North Atlantic SST pattern that is associated with the NAM. Second, no significant coherence is found at multidecadal time scale between the aforementioned North Atlantic SST pattern and North Pacific SST. Last, the PMV is virtually suppressed if the Rossby wave propagation in the North Pacific Ocean is blocked. More specifically, we have performed an additional sensitivity experiment whose setting is identical to the PC-ET, except that in the ocean component, a restoring boundary of climatological temperature and salinity is inserted in the North Pacific along 180° within the latitude band 10° – 60° N, and from the bottom to 100 m below the surface. Thereby, the westward oceanic Rossby waves hardly propagate through this restoring boundary. Such a model surgery has been termed as partial blocking (PB) and is described in detail in L02 and W03. The quasi-50-yr peak disappears in the results from this experiment, indicating the key role of oceanic dynamics in the North Pacific Ocean and the irrelevance of a pure Atlantic origin. Collectively, the

Atlantic variability is not the origin of the modeled PMV.

It should be pointed out that the conclusions drawn here are based on a linear argument, though nonlinearity may come into play when the PC surgery is applied. Nevertheless, the close correspondence between CTRL and PC-ET in many aspects suggests a secondary effect of nonlinear tropical–extratropical interactions, and hence lends credence to the results presented here. More evidence of large-scale air–sea interaction in the extratropics is needed to verify the coupling nature of the PMV in CCSM3. An investigation of the detailed mechanism is being undertaken and will be reported later.

Acknowledgments. This work is supported by NOAA and DOE. The technical and editorial help from Dr. Lixin Wu and Mr. Mark Marohl is much appreciated. We thank Dr. Shoshiro Minobe and two anonymous reviewers for their incisive and thorough comments. Thanks also to Drs. Dan Vimont, Eric DeWeaver, and Matthew Hitchman for insightful suggestions at various stages of this research.

REFERENCES

- Alexander, M. A., I. Bladé, M. Newman, J. R. Lanzante, N.-C. Lau, and J. D. Scott, 2002: The atmospheric bridge: The influence of ENSO teleconnections on air–sea interaction over the global oceans. *J. Climate*, **15**, 2205–2231.
- An, S.-I., and B. Wang, 2005: The forced and intrinsic low-frequency modes in the North Pacific. *J. Climate*, **18**, 876–885.
- Barlow, M., S. Nigam, and E. H. Berbery, 2001: ENSO, Pacific decadal variability, and U.S. summertime precipitation, drought, and streamflow. *J. Climate*, **14**, 2105–2128.
- Barnett, T. P., D. W. Pierce, M. Latif, D. Dommenges, and R. Saravanan, 1999: Interdecadal interactions between the tropics and midlatitudes in the Pacific basin. *Geophys. Res. Lett.*, **26**, 615–618.
- Barsugli, J. J., and D. S. Battisti, 1998: The basic effects of atmosphere–ocean thermal coupling on midlatitude variability. *J. Atmos. Sci.*, **55**, 477–493.
- Bretherton, C. S., C. Smith, and J. M. Wallace, 1992: An intercomparison of methods for finding coupled patterns in climate data. *J. Climate*, **5**, 541–560.
- , M. Widmann, V. P. Dymnikov, J. M. Wallace, and I. Bladé, 1999: The effective number of spatial degrees of freedom of a time-varying field. *J. Climate*, **12**, 1990–2009.
- Cayan, D. R., S. A. Kammerdiener, M. D. Dettinger, J. M. Caprio, and D. H. Peterson, 2001: Changes in the onset of spring in the western United States. *Bull. Amer. Meteor. Soc.*, **82**, 399–415.
- Chao, Y., M. Ghil, and J. C. McWilliams, 2000: Pacific interdecadal variability in this century’s sea surface temperatures. *Geophys. Res. Lett.*, **27**, 2261–2264.
- Collins, W. D., and Coauthors, 2006: The Community Climate System Model version 3 (CCSM3). *J. Climate*, **19**, 2122–2143.
- Czaja, A., and J. Marshall, 2000: On the interpretation of AGCMs response to prescribed time-varying SST anomalies. *Geophys. Res. Lett.*, **27**, 1927–1930.
- D’Arrigo, R., and Coauthors, 2005: Tropical–North Pacific climate linkages over the past four centuries. *J. Climate*, **18**, 5253–5265.
- Deser, C., and M. L. Blackmon, 1995: On the relationship between tropical and North Pacific sea surface temperature variations. *J. Climate*, **8**, 1677–1680.
- , A. S. Phillips, and J. W. Hurrell, 2004: Pacific interdecadal climate variability: Linkages between the tropics and the North Pacific during boreal winter since 1900. *J. Climate*, **17**, 3109–3124.
- Enfield, D. B., and A. M. Mestas-Nunez, 1999: Multiscale variabilities in global sea surface temperatures and their relationships with tropospheric climate patterns. *J. Climate*, **12**, 2719–2733.
- Fedorov, A. V., and S. G. Philander, 2000: Is El Niño changing? *Science*, **288**, 1997–2002.
- Frankignoul, C., P. Muller, and E. Zorita, 1997: A simple model of the decadal response of the ocean to stochastic wind forcing. *J. Phys. Oceanogr.*, **27**, 1533–1546.
- Garreaud, R. D., and D. S. Battisti, 1999: Interannual (ENSO) and interdecadal (ENSO-like) variability in the Southern Hemisphere tropospheric circulation. *J. Climate*, **12**, 2113–2123.
- Gu, D. F., and S. G. H. Philander, 1997: Interdecadal climate fluctuations that depend on exchanges between the tropics and extratropics. *Science*, **275**, 805–807.
- Hasselmann, K., 1976: Stochastic climate models. 1. Theory. *Tellus*, **28**, 473–485.
- Jin, F.-F., 1997: A theory of interdecadal climate variability of the North Pacific ocean–atmosphere system. *J. Climate*, **10**, 1821–1835.
- Kaplan, A., M. A. Cane, Y. Kushnir, A. C. Clement, M. B. Blumenthal, and B. Rajagopalan, 1998: Analyses of global sea surface temperature 1856–1991. *J. Geophys. Res.*, **103**, 18 567–18 590.
- Kirtman, B. P., 1997: Oceanic Rossby wave dynamics and the ENSO period in a coupled model. *J. Climate*, **10**, 1690–1704.
- Kleeman, R., J. P. McCreary, and B. A. Klinger, 1999: A mechanism for generating ENSO decadal variability. *Geophys. Res. Lett.*, **26**, 1743–1746.
- Kushnir, Y., W. A. Robinson, I. Bladé, N. M. J. Hall, S. Peng, and R. Sutton, 2002: Atmospheric GCM response to extratropical SST anomalies: Synthesis and evaluation. *J. Climate*, **15**, 2233–2256.
- Kwon, Y.-O., and C. Deser, 2007: North Pacific decadal variability in the Community Climate System Model version 2. *J. Climate*, **20**, 2416–2433.
- Latif, M., 2006: On North Pacific multidecadal climate variability. *J. Climate*, **19**, 2906–2915.
- , and T. P. Barnett, 1994: Causes of decadal climate variability over the North Pacific and North America. *Science*, **266**, 634–637.
- , and T. P. Barnett, 1996: Decadal climate variability over the North Pacific and North America: Dynamics and predictability. *J. Climate*, **9**, 2407–2423.
- Linsley, B. K., G. M. Wellington, and D. P. Schrag, 2000: Decadal sea surface temperature variability in the subtropical South Pacific from 1726 to 1997 A.D. *Science*, **290**, 1145–1148.
- Liu, Z., and S. Xie, 1994: Equatorward propagation of coupled air–sea disturbances with application to the annual cycle of the eastern tropical Pacific. *J. Atmos. Sci.*, **51**, 3807–3822.

- , and L. Wu, 2004: Atmospheric response to North Pacific SST: The role of ocean–atmosphere coupling. *J. Climate*, **17**, 1859–1882.
- , —, R. Gallimore, and G. Jacob, 2003: Search for the origins of Pacific decadal climate variability. *Geophys. Res. Lett.*, **29**, 1404, doi:10.1029/2001GL013735.
- , Y. Liu, L. Wu, and R. Jacob, 2007: Seasonal and long-term atmospheric responses to reemerging North Pacific Ocean variability: A combined dynamical and statistical assessment. *J. Climate*, **20**, 955–980.
- Lysne, J., P. Chang, and B. Giese, 1997: Impact of the extratropical Pacific on equatorial variability. *Geophys. Res. Lett.*, **24**, 2589–2592.
- Mann, M., and J. Lees, 1996: Robust estimation of background noise and signal detection in climatic time series. *Climatic Change*, **33**, 409–445.
- Mantua, N. J., S. R. Hare, Y. Zhang, J. M. Wallace, and R. C. Francis, 1997: A Pacific interdecadal climate oscillation with impacts on salmon production. *Bull. Amer. Meteor. Soc.*, **78**, 1069–1079.
- McPhaden, M. J., and D. X. Zhang, 2002: Slowdown of the meridional overturning circulation in the upper Pacific Ocean. *Nature*, **415**, 603–608.
- Minobe, S., 1997: A 50–70 year climatic oscillation over the North Pacific and North America. *Geophys. Res. Lett.*, **24**, 683–686.
- , 1999: Resonance in bidecadal and pentadecadal climate oscillations over the North Pacific: Role in climatic regime shifts. *Geophys. Res. Lett.*, **26**, 855–858.
- , 2000: Spatio-temporal structure of the pentadecadal variability over the North Pacific. *Prog. Oceanogr.*, **47**, 381–408.
- Nakamura, H., G. Lin, and T. Yamagata, 1997: Decadal climate variability in the North Pacific during the recent decades. *Bull. Amer. Meteor. Soc.*, **78**, 2215–2225.
- Neelin, J. D., and W. J. Weng, 1999: Analytical prototypes for ocean–atmosphere interaction at midlatitudes. Part I: Coupled feedbacks as a sea surface temperature dependent stochastic process. *J. Climate*, **12**, 697–721.
- Newman, M., 2007: Interannual to decadal predictability of tropical and North Pacific sea surface temperatures. *J. Climate*, **20**, 2333–2356.
- , G. P. Compo, and M. A. Alexander, 2003: ENSO-forced variability of the Pacific decadal oscillation. *J. Climate*, **16**, 3853–3857.
- Peng, S., W. A. Robinson, and M. P. Hoerling, 1997: The modeled atmospheric response to midlatitude SST anomalies and its dependence on background circulation states. *J. Climate*, **10**, 971–987.
- Pierce, D. W., T. P. Barnett, and M. Latif, 2000: Connections between the Pacific Ocean tropics and midlatitudes on decadal timescales. *J. Climate*, **13**, 1173–1194.
- , —, N. Schneider, R. Saravanan, D. Dommenges, and M. Latif, 2001: The role of ocean dynamics in producing decadal climate variability in the North Pacific. *Climate Dyn.*, **18**, 51–70.
- Quadrelli, R., and J. M. Wallace, 2004: A simplified linear framework for interpreting patterns of Northern Hemisphere wintertime climate variability. *J. Climate*, **17**, 3728–3744.
- Rodwell, M. J., D. P. Rowell, and C. K. Folland, 1999: Oceanic forcing of the wintertime North Atlantic Oscillation and European climate. *Nature*, **398**, 320–323.
- Rogers, J. C., 1981: The North Pacific Oscillation. *Int. J. Climatol.*, **1**, 39–57.
- Saravanan, R., and J. C. McWilliams, 1997: Stochasticity and spatial resonance in interdecadal climate fluctuations. *J. Climate*, **10**, 2299–2320.
- , and —, 1998: Advective ocean–atmosphere interaction: An analytical stochastic model with implications for decadal variability. *J. Climate*, **11**, 165–188.
- Schneider, N., A. J. Miller, and D. W. Pierce, 2002: Anatomy of North Pacific decadal variability. *J. Climate*, **15**, 586–605.
- Seager, R., Y. Kushnir, N. H. Naik, M. A. Cane, and J. Miller, 2001: Wind-driven shifts in the latitude of the Kuroshio–Oyashio Extension and generation of SST anomalies on decadal timescales. *J. Climate*, **14**, 4249–4265.
- Solomon, A., J. P. McCreary, R. Kleeman, and B. A. Klinger, 2003: Interannual and decadal variability in an intermediate coupled model of the Pacific region. *J. Climate*, **16**, 383–405.
- Thompson, D. W. J., and J. M. Wallace, 2000: Annular modes in the extratropical circulation. Part I: Month-to-month variability. *J. Climate*, **13**, 1000–1016.
- Timmermann, A., M. Latif, R. Voss, and A. Grötzner, 1998: Northern Hemispheric interdecadal variability: A coupled air–sea mode. *J. Climate*, **11**, 1906–1931.
- Torrence, C., and G. P. Compo, 1998: A practical guide to wavelet analysis. *Bull. Amer. Meteor. Soc.*, **79**, 61–78.
- Trenberth, K. E., and J. W. Hurrell, 1994: Decadal atmosphere–ocean variations in the Pacific. *Climate Dyn.*, **9**, 303–319.
- Vimont, D. J., D. S. Battisti, and A. C. Hirst, 2001: Footprinting: A seasonal connection between the tropics and mid-latitudes. *Geophys. Res. Lett.*, **28**, 3923–3926.
- , —, and —, 2002: Pacific interannual and interdecadal equatorial variability in a 1000-yr simulation of the CSIRO coupled general circulation model. *J. Climate*, **15**, 160–178.
- , J. M. Wallace, and D. S. Battisti, 2003: The seasonal footprinting mechanism in the Pacific: Implications for ENSO. *J. Climate*, **16**, 2668–2675.
- Weng, W. J., and J. D. Neelin, 1999: Analytical prototypes for ocean–atmosphere interaction at midlatitudes. Part II: Mechanisms for coupled gyre modes. *J. Climate*, **12**, 2757–2774.
- Wu, L., Z. Liu, R. Gallimore, R. Jacob, D. Lee, and Y. Zhong, 2003: Pacific decadal variability: The tropical Pacific mode and the North Pacific mode. *J. Climate*, **16**, 1101–1120.
- , —, C. Li, and Y. Sun, 2007: Extratropical control of recent tropical Pacific decadal climate variability: A relay teleconnection. *Climate Dyn.*, **28**, 99–112.
- Yang, H. J., Q. Zhang, Y. F. Zhong, S. Vavrus, and Z. Y. Liu, 2005: How does extratropical warming affect ENSO? *Geophys. Res. Lett.*, **32**, L01702, doi:10.1029/2004GL021624.
- Yeager, S. G., C. A. Shields, W. G. Large, and J. J. Hack, 2006: The low-resolution CCSM3. *J. Climate*, **19**, 2545–2566.
- Zhang, Q., H. Yang, Y. Zhong, and D. Wang, 2005: An idealized study of the impact of extratropical climate change on El Niño–Southern Oscillation. *Climate Dyn.*, **25**, 869–880.
- Zhang, Y., J. M. Wallace, and D. S. Battisti, 1997: ENSO-like interdecadal variability: 1900–93. *J. Climate*, **10**, 1004–1020.